Structural Biology and Molecular Biophysics

TRPML1 gating modulation by allosteric mutations and lipids

Ninghai Gan, Yan Han, Weizhong Zeng, Youxing Jiang

Howard Hughes Medical Institute and Department of Physiology, University of Texas Southwestern Medical Center, Dallas, Texas, USA • Department of Biophysics, University of Texas Southwestern Medical Center, Dallas, Texas, USA

Reviewed Preprint
v2 • September 30, 2024
Revised by authors

Reviewed Preprint
v1 • August 23, 2024

Abstract

Transient Receptor Potential Mucolipin 1 (TRPML1) is a lysosomal cation channel whose loss-of-function mutations directly cause the lysosomal storage disorder mucolipidosis type IV (MLIV). TRPML1 can be allosterically regulated by various ligands including natural lipids and small synthetic molecules and the channel undergoes a global movement propagated from ligand-induced local conformational changes upon activation. In this study, we identified a functionally critical residue, Tyr404, at the C-terminus of the S4 helix, whose mutations to tryptophan and alanine yield gain- and loss-of-function channels, respectively. These allosteric mutations mimic the ligand activation or inhibition of the TRPML1 channel without interfering with ligand binding and both mutant channels are susceptible to agonist or antagonist modulation, making them better targets for screening potent TRPML1 activators and inhibitors. We also determined the high-resolution structure of TRPML1 in complex with the $PI(4,5)P_2$ inhibitor, revealing the structural basis underlying this lipid inhibition. In addition, an endogenous phospholipid likely from sphingomyelin is identified in the $PI(4,5)P_2$-bound TRPML1 structure at the same hotspot for agonists and antagonists, providing a plausible structural explanation for the inhibitory effect of sphingomyelin on agonist activation.

eLife Assessment

Transient receptor potential mucolipin 1 (TRPML1) functions as a lysosomal ion channel whose variants are associated with lysosomal storage disorder mucolipidosis type IV. This **important** report describes local and global structural changes driven by binding of regulatory phospholipids and by mutations that allosterically cause gain or loss of channel function. Most of the claims related to the allosteric regulation of TRPML1 are **convincingly** supported by two new cryo-EM structures which are evaluated within the context of previously reported TRPML1 structures, and a proposed allosteric gating mechanism is partially supported by functional electrophysiology results.

https://doi.org/10.7554/eLife.100987.2.sa2

Introduction

Transient Receptor Potential Mucolipin 1 (TRPML1) is a Ca^{2+}-permeable, non-selective, lysosomal cation channel ubiquitously expressed in mammalian cells (Dong *et al*, 2008; LaPlante *et al*, 2002; Sun *et al*, 2000). TRPML1 plays critical roles in many important cellular activities including lipid accumulation (Shen *et al*, 2012), signaling transduction (Kilpatrick *et al*, 2016), lysosome trafficking (Venkatachalam *et al*, 2015), and autophagy (Scotto Rosato *et al*, 2019). The loss-of-function mutations in TRPML1 directly cause the lysosomal storage disorder mucolipidosis type IV (MLIV), a neurodegenerative disease characterized by abnormal neurodevelopment, retinal degeneration, and iron-deficiency anemia (Bargal *et al*, 2000; Bassi *et al*, 2000; Gan & Jiang, 2022; Nilius *et al*, 2007). Because of its physiological importance and direct disease association, TRPML1 has been extensively studied and is a potential target for drug development.

TRPML1 can be regulated by various ligands including both natural lipids and small synthetic molecules. The channel can be activated by the lysosome-specific phosphatidylinositol 3,5-bisphosphate ($PI(3,5)P_2$) (Dong *et al*, 2010), but inhibited by the plasma membrane-enriched $PI(4,5)P_2$ (Zhang *et al*, 2012). Given its pharmacological importance, many synthetic agonists and antagonists have been developed for TRPML1 activation and inhibition (Chen *et al*, 2014; Grimm *et al*, 2010; Samie *et al*, 2013; Shen *et al*., 2012). Interestingly, the mTOR (Mammalian target of rapamycin) inhibitor rapamycin and its derivatives can also synergistically activate TRPML1 with $PI(3,5)P_2$ (Gan *et al*, 2022; Zhang *et al*, 2019). Recent studies also suggest that sphingomyelin, a major membrane component, can also modulate the TRPML1 activation (Prat Castro *et al*, 2022; Shen *et al*., 2012).

Several TRPML1 channel structures in both open and closed conformations with various ligands have been determined (Chen *et al*, 2017; Fine *et al*, 2018; Gan *et al*., 2022; Schmiege *et al*, 2017; Schmiege *et al*, 2021), revealing some unique features of the TRPML1 channel. Firstly, all ligand-binding sites in the structures converge to two hot spots: The N-terminal poly-basic pocket for PIP_2 and the inter-subunit interface in the middle of the membrane between S5 and S6 for agonists, antagonists, and rapamycin (Fine *et al*., 2018; Gan *et al*., 2022; Schmiege *et al*., 2017; Schmiege *et al*., 2021) (**Figure 1a**). Secondly, all open TRPML1 structures are almost identical regardless of the activation stimuli. Thirdly, structural comparison between the open and closed conformation illustrates that TRPML1 gating is not merely a local conformational change but involves the global movement of almost the entire channel mediated by tight inter- and intra-subunit packing within the channel tetramer (**Movie supplement 1**). Finally, the necessity of global movement for channel activation underlies the allosteric regulation of TRPML1 by two distantly bound ligands - that is, the ligand-induced local conformational change at one site can propagate to the other site and thereby affect the binding of the other ligand (Gan *et al*., 2022). The high allostery of TRPML1 gating would allow us to design allosteric mutations that are remote from the channel pore but can still stabilize the channel in an open or closed state, mimicking the ligand activation or inhibition of the channel. To this end, we identified Tyr404 on the S4 helix as an allosteric site whose mutation can promote or inhibit TRPML1 gating. Furthermore, we also determined a high-resolution structure of $PI(4,5)P_2$- inhibited TRPML1 and demonstrated that in addition to competing against $PI(3,5)P_2$ activator for the same site, $PI(4,5)P_2$ also allosteric inhibits small molecule agonist by stabilize the channel in the closed conformation. Furthermore, the high-resolution $PI(4,5)P_2$-bound TRPML1 structure also revealed a bound phospholipid likely from sphingomyelin at the agonist/antagonist site, providing a plausible explanation for sphingomyelin inhibition of TRPML1.

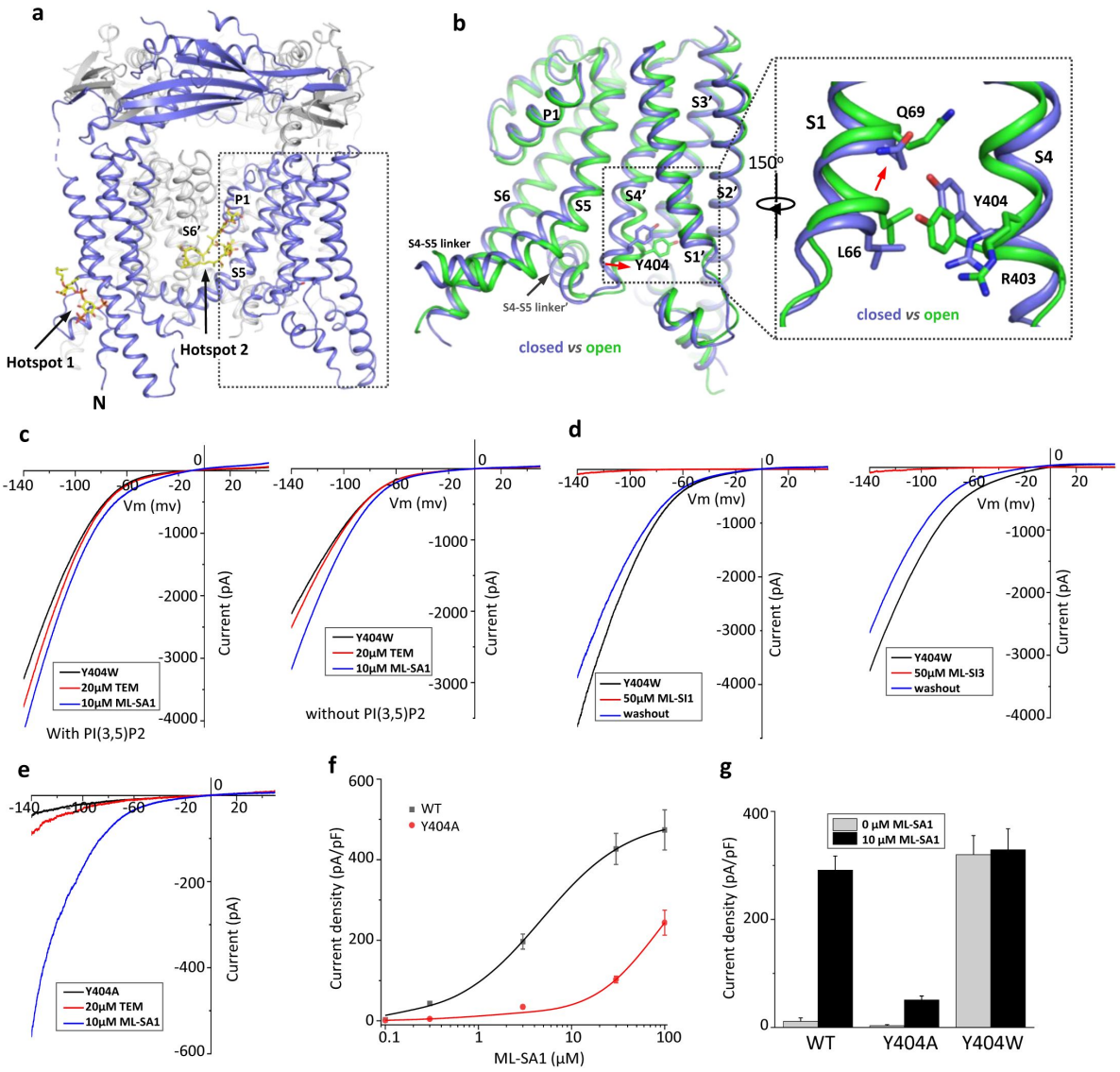

Figure 1

Design and characterization of allosteric mutations at Tyr404 that recapitulate TRPML1 gating.

(a) The structure of PI(3,5)P_2/Temsirolimus-activated TRPML1 (PDB code:7SQ9) illustrating the two hot spots for ligand binding. Temsirolimus (Tem) is a rapamycin analog. (b) Ligand-induced conformational change and the zoomed-in view of the Y404 movement. Only the boxed region in (a) is shown in the structural comparison between the open (green) and closed (blue) structures. Red arrows mark the bending of S4 and upward movement of S1. (c) Sample traces of Y404W gain-of-function mutant recorded using patch clamp in whole-cell configuration with (left) or without (right) 100 μM PI(3,5)P_2 in the pipette (cytosolic). Tem or agonist ML-SA1 was introduced in the bath solution (extracellular/luminal). (d) Sample traces of Y404W inhibition by antagonists ML-SI1 (left) and ML-SI3 (right) recorded using patch clamp in whole-cell configuration. The antagonists were introduced in the bath solution (extracellular/luminal). (e) Sample traces of Y404A loss-of-function mutant with 100 μM PI(3,5)P_2 in the pipette (cytosolic). Tem or ML-SA1was introduced in the bath solution (extracellular/luminal). (f) ML-SA1 activation of TRPML1(WT) and Y404A mutant measured at -140 mV. Data for WT is least square fits to the Hill equation with EC_{50}=4.8±0.7 μM, n=0.93±0.10. Data points are mean ± SEM (n=5 independent experiments). (f) Current density of wild-type and mutant TRPML1 at -140mV with and without 10μM ML-SA1. Data points are mean ± SEM (n=5 independent experiments)

Results

Allosteric mutations at Tyr404 recapitulate TRPML1 gating

Our previous study on the allosteric activation of TRPML1 by $PI(3,5)P_2$ and rapamycin demonstrated that ligand-induced local conformational changes can propagate to distal parts of the channel through tight inter- and intra-subunit packing within the channel tetramer, allowing the channel to integrate the stimuli from these two distantly bound ligands. The $PI(3,5)P_2$ and rapamycin-induced local conformational changes converge to the same driving force on S4 helix, resulting in a slight bend of the C-terminal half of the S4 that facilitates the channel opening (Gan *et al*., 2022) (**Figure 1b**). A key interaction coupled to the S4 bending movement is the insertion of Tyr404 side chain into a pocket surrounded by S1, S3, and S4 helices where its aromatic ring is sandwiched between the side chains of Leu66 and Arg403. We hypothesized that mutations at Tyr404 that stabilize its sidechain in the pocket would facilitate channel activation; conversely, mutations that destabilize its sidechain in the pocket would negatively modulate the channel activation. To test this, we replaced Tyr404 with tryptophan and alanine, respectively, and measured the effect of these mutations on channel activity. As illustrated in the electrophysiological recordings using whole-cell patches, the Y404W mutant elicits large inward-rectifying currents without any ligands, indicating that Y404W is a gain-of-function (GOF) mutant (**Figure 1c** and **Figure supplement 1a**). Adding extra activation ligands such as $PI(3,5)P_2$, rapamycin, or small molecule agonist ML-SA1 only marginally increases the currents. The Y404W GOF mutant mimics a ligand-activated channel, yet its mutation site is remote from the pore domain and the channel can still be allosterically inhibited by small molecule antagonists (ML-SI1 and ML-SI3) (**Figure 1d** and **Figure supplement 1b**). This is distinct from other gain-of-function mutants in which proline substitutions on the S5 helix lock the pore in an open state and the channels are no longer susceptible to antagonist inhibition (Dong *et al*, 2009; Grimm *et al*, 2007; Kim *et al*, 2007; Nagata *et al*, 2008; Xu *et al*, 2007).

Y404A, on the other hand, represents a loss-of-function mutant and elicits much lower currents even in the presence of potent agonist ML-SA1 (**Figure 1e** and **Figure supplement 1c**). While ML-SA1 can potently activate the wild-type TRPML1 channel, the Y404A mutation mimics $PI(4,5)P_2$ inhibition and allosterically inhibits ML-SA1 binding, significantly decreasing the efficacy of ML-SA1 activation (**Figure 1f** & g).

Structure of GOF Y404W mutant

To reveal the structural basis underlying the channel activation of the Y404W mutant, we determined its structure in the absence of any ligands to 2.86 Å resolution (**Figure supplement 2-3** and Methods). As expected, the Y404W mutant adopts an open conformation with a structure almost identical to other ligand-activated open TRPML1, consistent with its GOF property (**Figure 2a** and **Figure supplement 3b**). Like Tyr404 in the wide-type open TRPML1, the side chain of W404 in the mutant is inserted into the pocket surrounded by S1, S3, and S4 helices and sandwiched between Leu66 and Arg403 (**Figure 2b**). However, the larger indole ring of Trp404 provides a better spatial fitting into the pocket than the phenol ring of Tyr404 and several surrounding residues (Lys65, Gln69, and Leu358) provide extra van der Waals contacts to the Trp404 side chain. Thus, by enhancing the stability of the aromatic side chain inside the pocket, Y404W mutation facilitates the bending of S4 which in turn propagates to the pore through the S4-S5 linker and activates the channel (Gan *et al*., 2022). The Y404W mutant structure demonstrates that the sidechain packing in the pocket is essential for stabilizing the open channel and the lack of such packing capacity in the Y404A mutant with a small side-chain likely destabilizes the open conformation, yielding a loss-of-function channel. It is worth noting that Arg403 plays two essential roles in TRPML1 gating: its side chain is part of the pocket that stabilizes Tyr404 in the open state; its guanidinium group forms a salt bridge with the C3 phosphate group of $PI(3,5)P_2$

upon ligand activation (Gan *et al*., 2022). As expected, Arg403 is highly conserved in the TRPML channel family, and its R403C variant identified in an MLIV patient is a loss-of-function mutant (Chen *et al*., 2014).

Structure of TRPML1 in PI(4,5)P_2-bound closed state

While PI(4,5)P_2 inhibits PI(3,5)P_2 activation of TRPML1 by directly competing for the same binding site, it also allosterically inhibits the agonist-activated channel (Chen *et al*., 2017), suggesting that PI(4,5)P_2 binding stabilizes the TRPML1 channel in a closed conformation. A previous low-resolution structure of TRPML1 in complex with PI(4,5)P_2 revealed the approximate location of PI(4,5)P_2 binding but failed to explain how its binding stabilizes the channel in the closed state and allosterically inhibits the agonist-activated channel (Fine *et al*., 2018). To address this, we determined the structure of PI(4,5)P_2-bound TRPML1 at 2.46 Å (**Figure 3a**, **Figure supplement 3**-**5** and Methods). The density from the IP3 head group of PI(4,5)P_2, especially the phosphate groups on C4 and C5 of the inositol, can be clearly defined in the EM map (**Figure 3a**-**3c**). The phosphatidyl group, however, is flexible and could not be resolved in the structure. While PI(4,5)P_2 binding overlaps with that of PI(3,5)P_2, their IP3 head group positions are quite different (**Figure 3b**-**3e**). In the PI(3,5)P_2-bound structure (**Figure 3d**), the head group protrudes deep into the N-terminal PIP_2-binding pocket enclosed by two short clamp-shaped helices of H1 and H2, and the cytosolic ends of S1 and S2 helices, allowing its C3 phosphate to engage in direct interactions with Arg403 and Tyr355 to facilitate channel activation (Gan *et al*., 2022). These C3 phosphate-mediated interactions are absent in PI(4,5)P_2-bound structure. Instead, the head group of PI(4,5)P_2 is trapped at the entrance of the pocket and forms a bridge between S1 and S2 with its phosphate groups stabilized by positively charged residues from H2, S1, and S2 (**Figure 3b** & **3c**). A major conformational change between the open and closed states is an upward movement of the S1 helix, a prerequisite for Tyr404 insertion between Leu66 and Arg403 and the subsequent bending of S4 (**Figure 3e**). Therefore, the PI(4,5)P_2-mediated bridging interaction between S1 and S2 would hinder the S1 movement and stabilize the channel in the closed conformation, exerting allosteric inhibition on agonist activation.

Endogenous sphingomyelin lipid at the agonist- and antagonist-binding site

The high-resolution structure of PI(4,5)P_2-bound closed TRPML1 also reveals a well-defined density from an endogenous lipid molecule at the inter-subunit interface between S5 and S6 (**Figure 4a**). The lipid contains a choline head group and is likely a phosphatidylcholine (PC) or sphingomyelin (SM), the two main choline-containing phospholipid components of the outer leaflet of the plasma membrane. The tail from one of the lipid alkyl chains penetrates deep into an inter-subunit pocket in the middle of the membrane, overlapping with the hotspot for both channel agonist and antagonist (**Figure supplement 6**). This alkyl chain has to be displaced upon agonist or antagonist binding, suggesting that the lipid occupation would compete against agonist or antagonist binding. We suspect this bound lipid is sphingomyelin which is also enriched in the endocytic recycling compartment and has been shown to inhibit TRPML1 activity (Prat Castro *et al*., 2022; Schuchman, 2010; Shen *et al*., 2012; Slotte, 2013). Key evidence to support SM inhibition is that its enrichment can reduce the agonist (i.e. SF-51 and ML-SA1) activation of TRPML1 (Shen *et al*., 2012). Indeed, we did observe the reduction of SF-51-activated TRPML1 current upon SM enrichment (**Figure 4b** and **Figure supplement 7a**). However, based on our structure, we hypothesize that the role of sphingomyelin is to stabilize rather than directly inhibit the channel; the SM inhibition upon enrichment is an indirect effect attributable to its competition against agonist binding that reduces the apparent efficacy of agonist activation. This hypothesis would imply that SM can also function as an indirect activator by competing against antagonists and reducing their effectiveness in channel inhibition. The gain-of-function Y404W mutant, which is still susceptible to antagonist inhibition, provides a good system to test

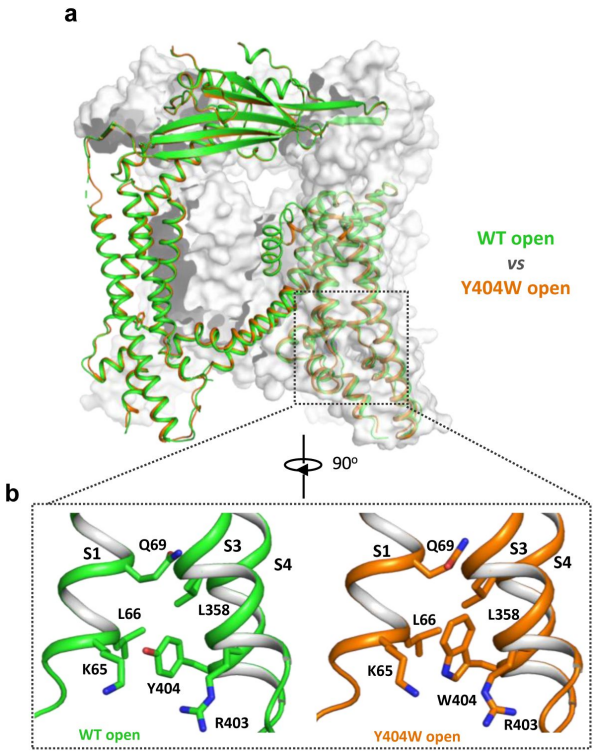

Figure 2.

Y404W mutant adopts an open conformation in the absence of ligands.

(a) Structural comparison between PI(3,5)P_2/Tem-bound open structure (green) and the Y404W mutant structure (orange). Only the front subunit and the neighboring S1-S4 regions are highlighted in color for clarity. (b) Zoomed-in views of the regions surrounding Y404 (WT, green) and W404 (mutant, orange).

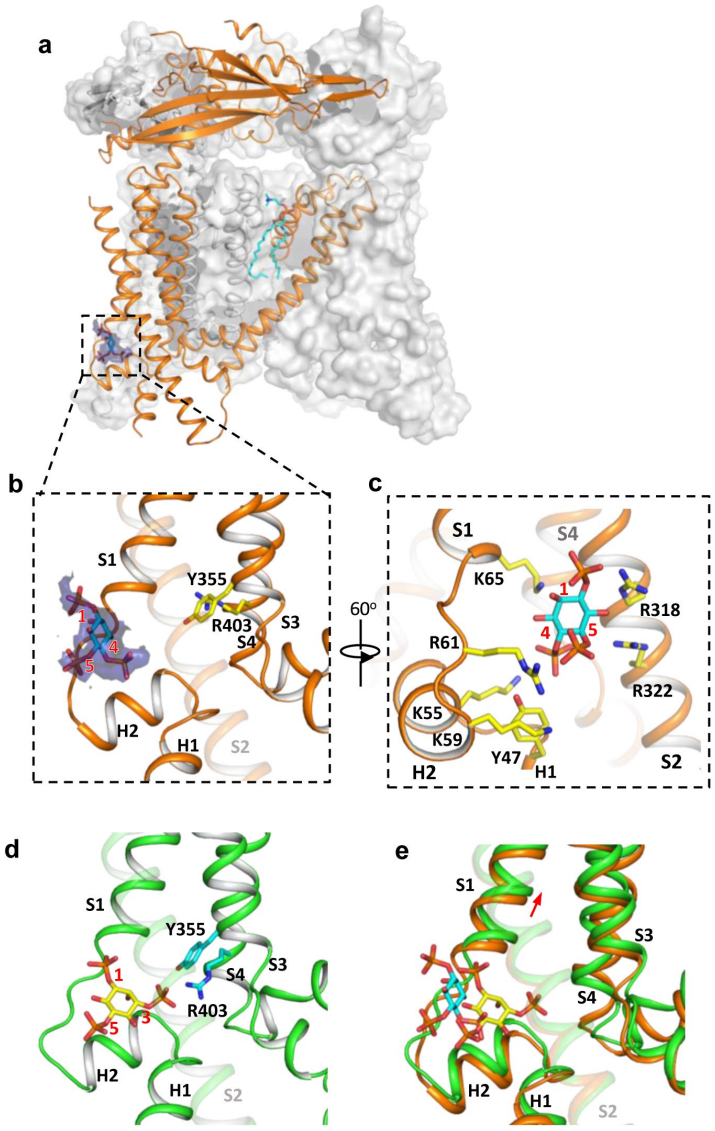

Figure 3.

Structure of TRPML1 in complex with PI(4,5)P_2.

(a) Overall structure of PI(4,5)P_2-bound TRPML1 with the front subunit shown in orange cartoon and the rest shown as grey surface representation. Density for PI(4,5)P_2 head group is shown in blue surface. (b) Zoomed-in view of the PI(4,5)P_2-binding pocket with the density of its IP3 head group shown in blue surface. (c) Zoomed-in view of the PI(4,5)P_2-binding pocket with side chains of IP3-interacting residues shown as yellow sticks. (d) Zoomed-in view of the IP3 position in the PI(3,5)P_2-bound open TRPML1 structure. The C3 phosphate group directly interacts with Y355 and R403. (e) Comparison of the head group positions in PI(3,5)P_2-bound open (green) and PI(4,5)P_2-bound closed (orange) structures. The inositol rings PI(3,5)P_2 and PI(4,5)P_2 are colored yellow and cyan, respectively. The red arrow marks the upward movement of S1 from closed to open conformation.

that. As shown in **Figure 4c** and **Figure supplement 7b**, SM shows no obvious inhibition to the mutant channel activity whereas antagonist ML-SI1 markedly reduces the mutant channel current; upon SM enrichment, ML-SI1 inhibition is mitigated resulting in a recovery of the channel current. This observation confirms the competitive binding of SM at the hot spot for both agonists and antagonists.

Summary

In this study, we designed and analyzed the allosteric mutations at Tyr404 that recapitulate the gating of TRPML1. Replacing this tyrosine with tryptophan or alanine stabilizes or destabilizes the channel in the open state, yielding a gain- or loss-of-function mutant. The structure of the Y404W mutant adopts the same open structure as ligand-activated TRPML1, once again highlighting the global conformational change for TRPML1 channel activation. As Tyr404 is distant from the hot spots for ligand binding, the two gain- and loss-of-function mutants can still be allosterically modulated by antagonists and agonists. Thus, these allosteric mutants can mimic ligand-activated or inhibited TRPML1 without interfering with ligand binding, making them better targets for screening potent small molecule TRPML1 inhibitors and activators. We also investigated the structural basis of $PI(4,5)P_2$ inhibition of TRPML1 by determining the $PI(4,5)P_2$- bound structure, revealing a different binding mode by its head group at the N-terminal polybasic site than that of $PI(3,5)P_2$. The head group of $PI(4,5)P_2$ mediates a bridging interaction between S1 and S2 and stabilizes TRPML1 in a closed conformation. In the high-resolution $PI(4,5)P_2$- bound TRPML1 structure, we also visualize clear density from a choline-containing phospholipid at the same site for agonists or antagonists. In light of its high membrane abundance and competing effect on agonist activation and antagonist inhibition, this bound lipid is likely from sphingomyelin.

Methods

Protein expression and purification

Protein expression and purification were performed as previously described (Gan *et al*., 2022). The *Mus musculus* TRPML1 gene with a C-terminal thrombin cleavage site and a 10× His tag was cloned into a pEZTBM vector (Morales-Perez *et al*, 2016) and heterologously expressed in HEK293F cells using the BacMam system. The baculovirus was produced in Sf9 cells and used to transduce the HEK293F cells at a ratio of 1:40 (virus:HEK293F, v/v) and supplemented with 1 mM sodium butyrate to boost the protein expression. Cells were cultured in suspension at 37 °C for 48 h and harvested by centrifugation at 3,000*g*. All purification procedures were carried out at 4 °C unless specified otherwise. The cell pellet was re-suspended in buffer A (20 mM Tris pH 8.0, 150mM NaCl) supplemented with a pro0tease inhibitor cocktail (containing 1 mg ml−1 each of DNase, pepstatin, leupeptin, and aprotinin and 1 mM PMSF) and homogenized by sonication on ice. Protein was extracted with 1% (w/v) n-dodecyl-β-D-maltopyranoside (DDM; Anatrace) supplemented with 0.2% (w/v) cholesteryl hemisuccinate (CHS; Sigma-Aldrich) by gentle agitation for 2 h. After extraction, the supernatant was collected after a 1 h centrifugation at 48,000g and incubated with Ni-NTA resin and 20 mM imidazole with gentle agitation. After 1 h, the resin was collected on a disposable gravity column (Bio-Rad), washed with buffer B (buffer A + 0.04%glyco-diosgenin (GDN; Anatrace)) with 20 mM imidazole. The washed resin was left on-column in buffer B and digested with thrombin overnight. After digestion, the flow-through was concentrated, and purified by size-exclusion chromatography on a Superose 6 10/300 GL column (GE Heathcare) pre-equilibrated with buffer B. The protein peak was collected and concentrated. For $PI(4,5)P_2$-bound structure, purified protein was incubated with 0.5mM $PI(4,5)P_2$ on ice for 4 h. The lipid ligand used in this study is $PI(4,5)P_2$ diC8 (Echelon)

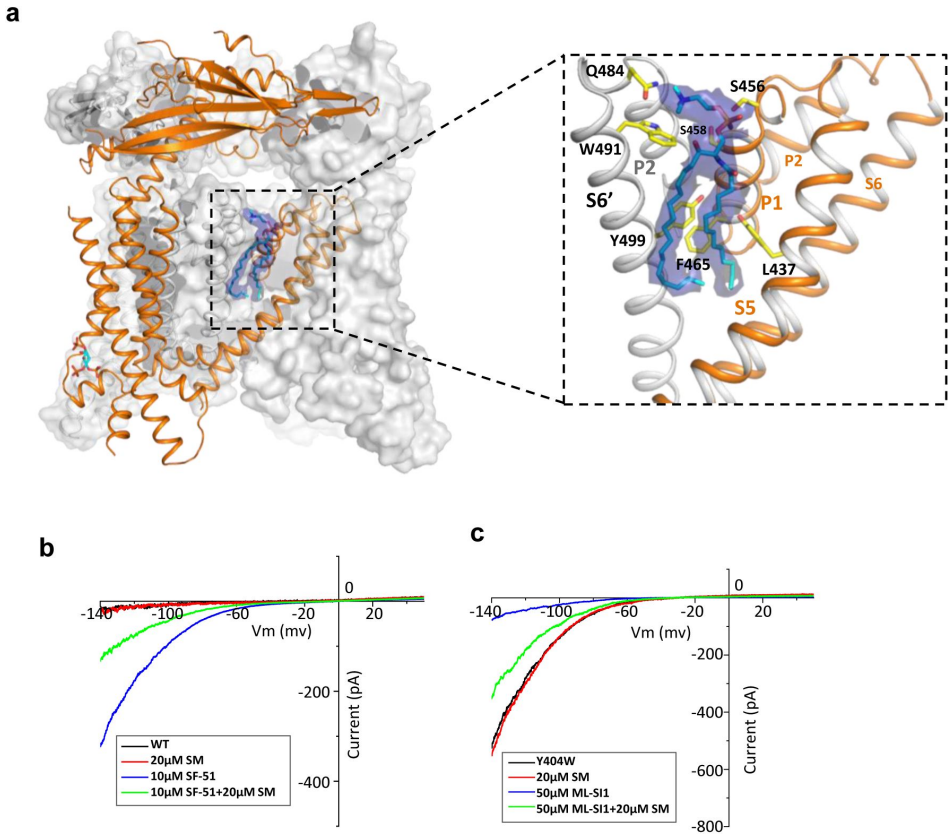

Figure 4.

Sphingomyelin binding in TRPML1.

(a) Overall structure of PI(4,5)P_2-bound TRPML1 and the zoomed-in view of the lipid-binding site. The lipid density is shown as blue surface and modeled as sphingomyelin (SM). The side chains of lipid-interacting residues are shown as yellow sticks. (b) SM inhibition effect on SF-51-activated wild-type TRPML1. (c) SM activation effect on ML-SI1-inhibited Y404W mutant. Currents shown in (b) and (c) were recorded using patch clamp in whole-cell configuration with pH 4.6 in the bath solution as the adverse effect of SM on agonist or antagonist is subtle and is measurable only at low luminal pH.

Electron microscopy data acquisition

Electron microscopy data acquisition followed the protocol previously described (Gan *et al*., 2022). The cryo-EM grids were prepared by applying 3.5 µl protein (3.5 mg/mL) to a glow-discharged Quantifoil R1.2/1.3 200-mesh copper holey carbon grid (Quantifoil, Micro Tools GmbH) and blotted for 3.0 s under 100% humidity at 4 °C before being plunged into liquid ethane using a Mark IV Vitrobot (FEI). For the dataset of Y404W, micrographs were acquired on a Titan Krios microscope (FEI) operated at 300 kV with a K3 Summit direct electron detector (Gatan), using a slit width of 20 eV on a GIF-Quantum energy filter. Data were collected using CDS (Correlated Double Sampling) mode of the K3 camera with a super resolution pixel size of 0.413 Å. The defocus range was set from −0.9 to −2.2 µm. Each movie was dose-fractionated to 60 frames with a dose rate of 1e-/Å^2/frame for a total dose of 60e-/Å^2. The total exposure time was between 5 to 6 s. For the PI(4,5)P_2-bound dataset, micrographs were acquired on a Titan Krios microscope (FEI) operated at 300 kV with a Falcon4 electron detector (Thermo Fisher), using a slit width of 20 eV on a post-column Selectris X energy filter (Thermo Fisher Scientific). Data was collected using Falcon 4 camera with a pixel size of 0.738 Å. The defocus range was set from -0.9 to -2.2 µm. Each movie was dose-fractionated to 60 frames with a dose rate of 1e-/Å^2/frame for a total dose of 60e-/Å^2. The total exposure time was between 3.5 to 4 s.

Image processing

Images were processed as previously described (Gan *et al*., 2022). Movie frames were motion corrected and binned two times and dose-weighted using MotionCor2 (Zheng *et al*, 2017). The CTF parameters of the micrographs were estimated using the GCTF program (Zhang, 2016). The rest of the image processing steps were carried out using RELION 3.1 (Nakane *et al*, 2020; Scheres, 2012; Zivanov *et al*, 2018). All resolution was reported according to the gold-standard Fourier shell correlation (FSC) using the 0.143 criterion (Henderson *et al*, 2012). Local resolution was estimated using Relion. Aligned micrographs were manually inspected to remove those with ice contamination and bad defocus. Particles were selected using Gautomatch (K. Zhang, MRC LMB, *https://www2.mrc-lmb.cam.ac.uk/research/locally-developed-software/zhang-software/*) and extracted using a binning factor of 3. 2D classification was performed in Relion 3.1. Selected particles after 2D classification were subjected to one around 3D classification. The mouse TRPML1 map (EMD-8883 (Chen *et al*., 2017)) low-pass filtered to 30 Å was used as the initial reference. Classes that showed clear features of the TRPML1 channel were combined and subjected to 3D auto-refinement and another round of 3D classification without performing particle alignment using a soft mask around the protein portion of the density. The best resolving classes were then re-extracted with the original pixel size and further refined. Beam tilt, anisotropic magnification, and per-particle CTF estimations and Bayesian polishing were performed in Relion 3.1 to improve the resolution of the final reconstruction.

For the Y404W structure dataset, a total of 4,724 movies were collected and 4,505 were selected after motion correction and CTF estimation. A total number of 864,698 particles were extracted from the selected micrographs and were subjected to one round of 2D classification, from which 87,846 particles were selected. After the initial 3D classification, 35,460 particles were selected and subjected to a 3D auto-refinement job and further ctf refinements, yielding a map at 2.86Å overall resolution (**Figure supplement 2**).

For the PI(4,5)P_2-bound dataset, a total of 8,164 movies were collected and 7,895 were selected after motion correction and CTF estimation. A total number of 1,065,778 particles were extracted from the selected micrographs and were subjected to one round of 2D classification, from which 555,281 particles were selected. After the initial 3D classification, 359,441 particles were selected and subjected to a 3D auto-refinement job. Next, a soft mask excluding the micelle density was applied and particles were sorted into 5 classes without performing alignment. From this, one

classe with a total number of 60,597 particles were selected and further refined. In the postprocess step, a B-factor of -60 was manually given, yielding a map at 2.46Å overall resolution (**Figure supplement 4**).

Model building, refinement and validation

Model building, refinement and validation followed the previously described protocol (Gan *et al*., 2022). The structure of mouse TRPML1 (PDB code: 5WPV) was used as the initial model and was manually adjusted in Coot (Emsley *et al*, 2010) and refined against the map by using the real space refinement module with secondary structure and non-crystallographic symmetry restraints in the Phenix package (Adams *et al*, 2010). The final structure model of Y404W includes residues 40-200, 216-527. The final structure model of the PI(4,5)P_2-bound includes residues 39-200, 216-285, 296-527. About 40 residues at the amino terminus and 50 residues at the carboxy terminus are disordered and not modeled. The statistics of the geometries of the models were generated using MolProbity (Chen *et al*, 2010). All the figures were prepared in PyMol (Schrödinger, LLC.), UCSF Chimera (Pettersen *et al*, 2004). Pore radii were calculated using the HOLE program(Smart *et al*, 1996).

Electrophysiology

Electrophysiology was carried out following a previously described protocol with minor modifications (Gan *et al*., 2022). For electrophysiological analysis, the two di-leucine motifs (15_{LL} and 577_{LL}) of mouse TRPML1 responsible for lysosomal targeting were replaced with alanines to facilitate the trafficking of the channel to the plasma membrane (Grimm *et al*., 2010; Vergarajauregui & Puertollano, 2006). The N-terminal GFP tagged, plasma membrane-targeting TRPML1 mutant (TRPML1-4A) and derived point mutations were overexpressed in HEK293 cells and the channel activities were directly measured by patching the plasma membrane. In this setting, the extracellular side is equivalent to the luminal side of TRPML1 in endosomes or lysosomes. 48 h after transfection, cells were dissociated by trypsin treatment and kept in complete serum-containing medium; the cells were re-plated onto 35 mm tissue culture dishes and kept in a tissue culture incubator until recording. Patch clamp in the whole-cell or inside-out configuration was used to measure TRPML1 activity on the HEK plasma membrane. The standard bath solution for whole cell current recording contained (in mM): 145 sodium methanesulfonate, 5 NaCl, 1 $MgCl_2$, 10 HEPES buffered with Tris, pH 7.4; and the pipette solution contained (in mM): 140 caesium methanesulfonate, 5 NaCl, 5 $MgCl_2$, 10 EGTA, 10 HEPES buffered with Tris, pH 7.4. The bath solution for inside-out configuration contained (in mM): 140 potassium methanesulfonate, 5 NaCl, 2 $MgCl_2$, 0.4 $CaCl_2$, 1 EGTA, 10 HEPES buffered with Tris, pH 7.4; and the pipette solution contained (in mM): 145 sodium methanesulfonate, 5 NaCl, 1 $MgCl_2$, 0.5 EGTA, 10 HEPES buffered with Tris, pH 7.4. For whole cell recording of PI(3,5)P_2-activated channel, we had to include high concentration of PI(3,5)P_2 (100 μM) in the pipette solution (cytosolic side) in order to quickly obtain stable PI(3,5)P_2-evoked current, likely because of the slow diffusion of this lipid ligand. PI(4,5)P_2 was added in the cytosolic side, Tem, ML-SA1, ML-SI3, ML-SI1, SM were added in the bath solution. SM competition assays with SF-51 and ML-SI1 were conducted under pH 4.6. The patch pipettes were pulled from Borosilicate glassand heat polished to a resistance of 2–5 MΩ (2–3 MΩ for inside-out patch, and 3–5 MΩ for whole-cell current recoding). Data were acquired using an AxoPatch 200B amplifier (Molecular Devices) and a low-pass analogue filter set to 1 kHz. The current signal was sampled at a rate of 20 kHz using a Digidata 1550B digitizer (Molecular Devices) and further analyzed with pClamp 11 software (Molecular Devices). After the patch pipette attached to the cell membrane, the giga seal (>10 GΩ) was formed by gentle suction. The inside-out configuration was formed by pulling the pipette away from the cell, and the pipette tip was exposed to the air for 2 seconds. The whole-cell configuration was formed by short zap or suction to rupture the patch. The holding potential was set to 0 mV. The whole-cell and inside-out macroscopic current recordings were obtained using voltage pulses ramped from −140 mV to +50

mV over a duration of 800 ms. The sample traces for the I–V curves of macroscopic currents shown in each figure were obtained from recordings on the same patch. All data points are mean ± s.e.m. ($n \geq 5$).

Data availability

The cryo-EM density maps of mouse TRPML1 have been deposited in the Electron Microscopy Data Bank (EMDB) under accession numbers 45429 (Y404W), 45432 (PI(4,5)P_2-bound). Atomic coordinates have been deposited in the Protein Data Bank (PDB) under accession numbers 9CBZ (Y404W), 9CC2 (PI(4,5)P_2-bound).

Acknowledgements

Cryo-EM sample grids were prepared at the Structural Biology Laboratory at the University of Texas Southwestern Medical Center which is partially supported by the CPRIT Core Facility Support Award RP170644. Single particle Cryo-EM data were collected at the University of Texas Southwestern Medical Center Cryo-EM Facility that is funded by the CPRIT Core Facility Support Award RP170644 and Pacific Northwest Center for Cryo-EM (PNCC). We thank Omar Davulcu for helping in data collection at PNCC under user proposal 51776. Ninghai Gan is a HHMI fellow of the Jane Coffin Childs Memorial Fund. This work was supported in part by the Howard Hughes Medical Institute and by grants from the National Institute of Health (R35GM140892 to Y.J.) and the Welch Foundation (Grant I-1578 to Y.J.).

Author contributions

N.G. prepared the samples; Y.H. and N.G. performed data acquisition, image processing, and structure determination; W.Z. performed electrophysiology recording; All authors participated in research design, data analysis, discussion, and manuscript preparation.

Declaration of interests

The authors declare no competing financial interests

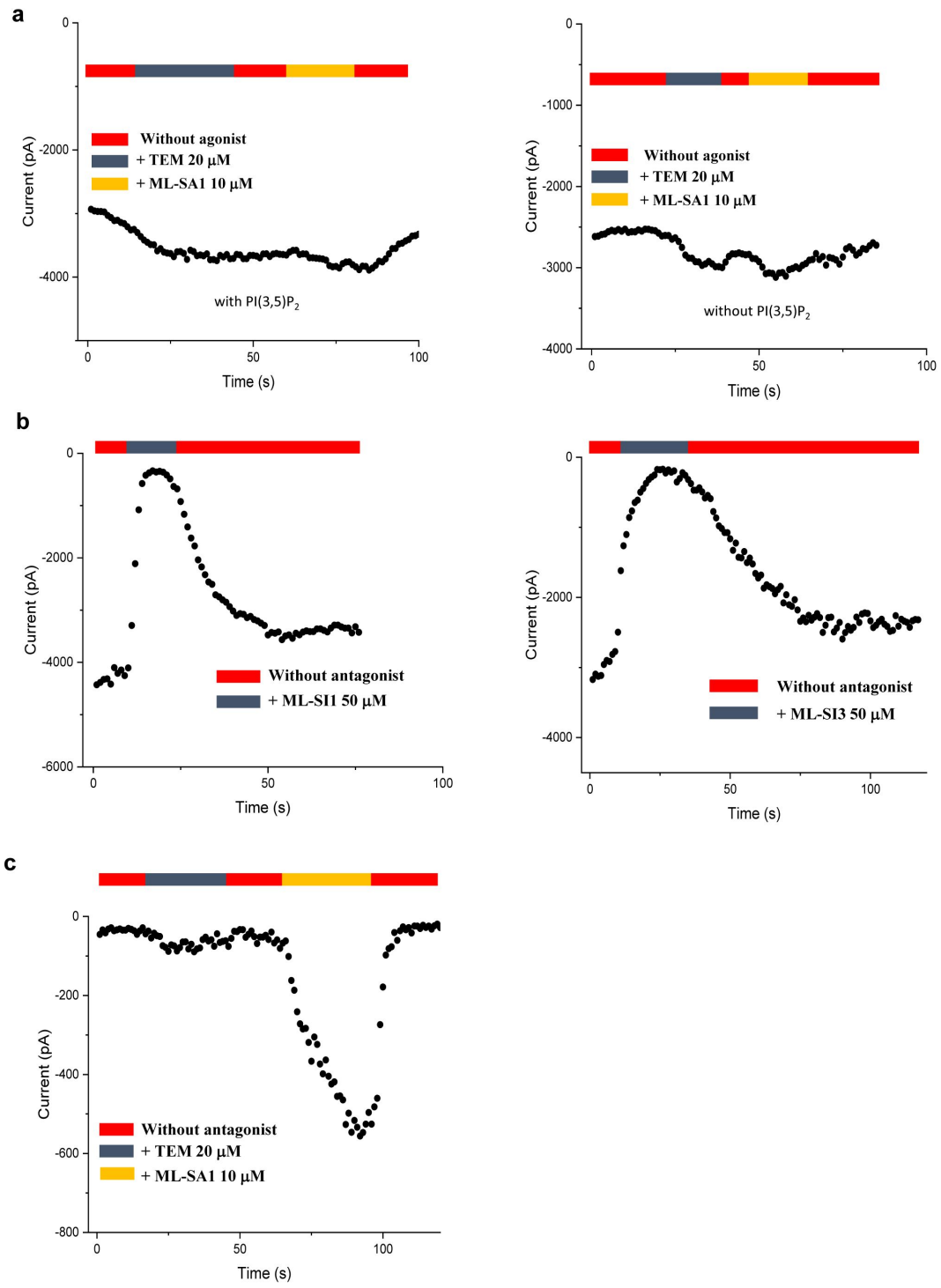

Figure supplement 1

Time course plots of current amplitudes of Y404 mutations recorded at -140mV with symmetrical pH of 7.4.

(a) Time course plots of Y404W recorded using patch clamp in whole-cell configuration with (left) or without (right) 100 μM $PI(3,5)P_2$ in the pipette (cytosolic). Tem or agonist ML-SA1 was introduced in the bath solution (extracellular/luminal). (b) Time course plots of Y404W inhibition by antagonists ML-SI1 (left) and ML-SI3 (right) recorded using patch clamp in whole-cell configuration. The antagonists were introduced in the bath solution (extracellular/luminal). (c) Time course plots of Y404A with 100 μM $PI(3,5)P_2$ in the pipette (cytosolic). Tem or ML-SA1was introduced in the bath solution (extracellular/luminal).

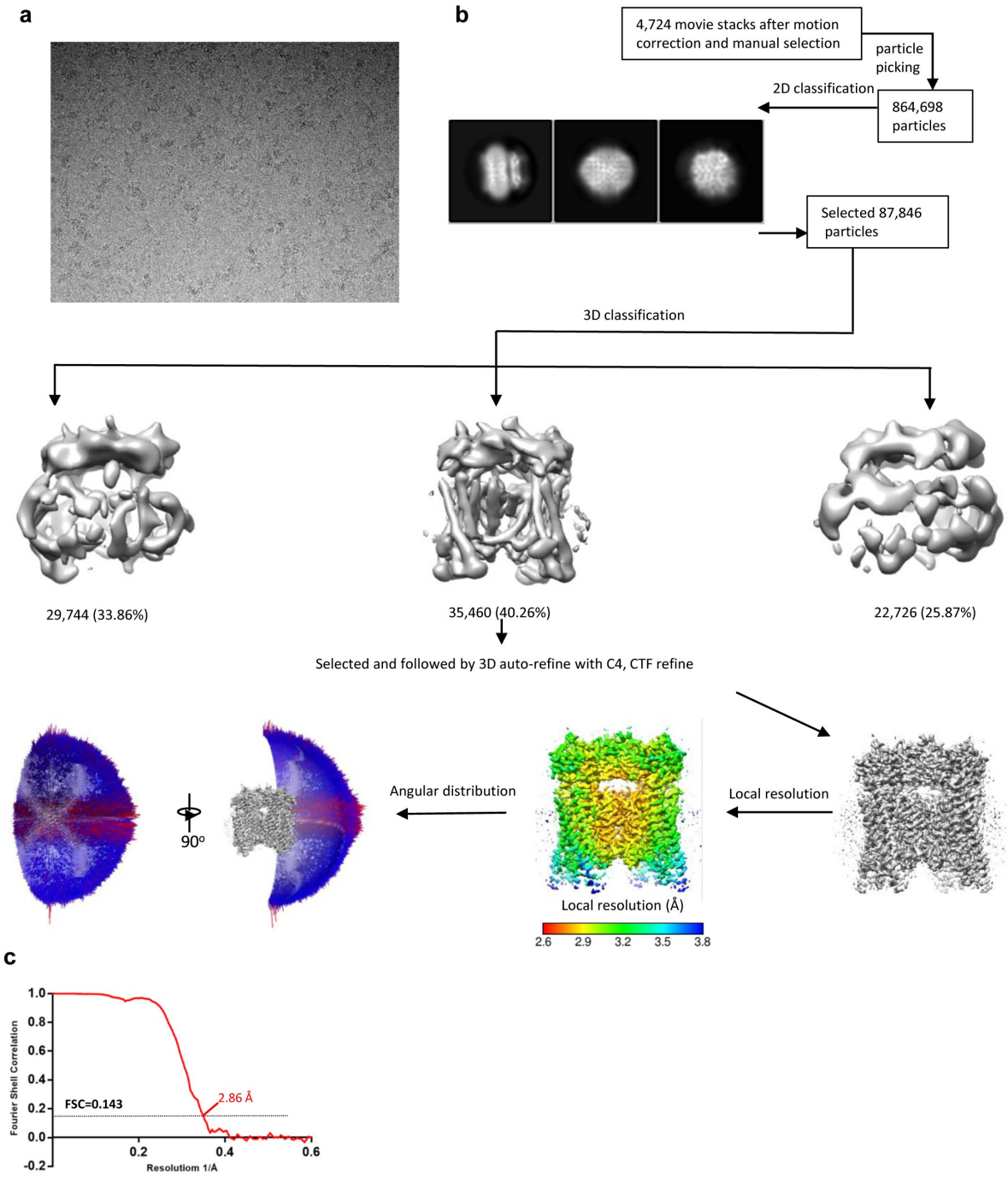

Figure supplement 2

Cryo-EM data processing scheme of the TRPML1 Y404W.

(a) Representative micrograph. (b) Flow chart of the cryo-EM data processing procedure and the Euler angle distribution of particles used in the final three-dimensional reconstruction. Selected 2D class averages are shown. The final structure represent an open state. (c) Fourier Shell Correlation curves showing the overall resolution at FSC=0.143.

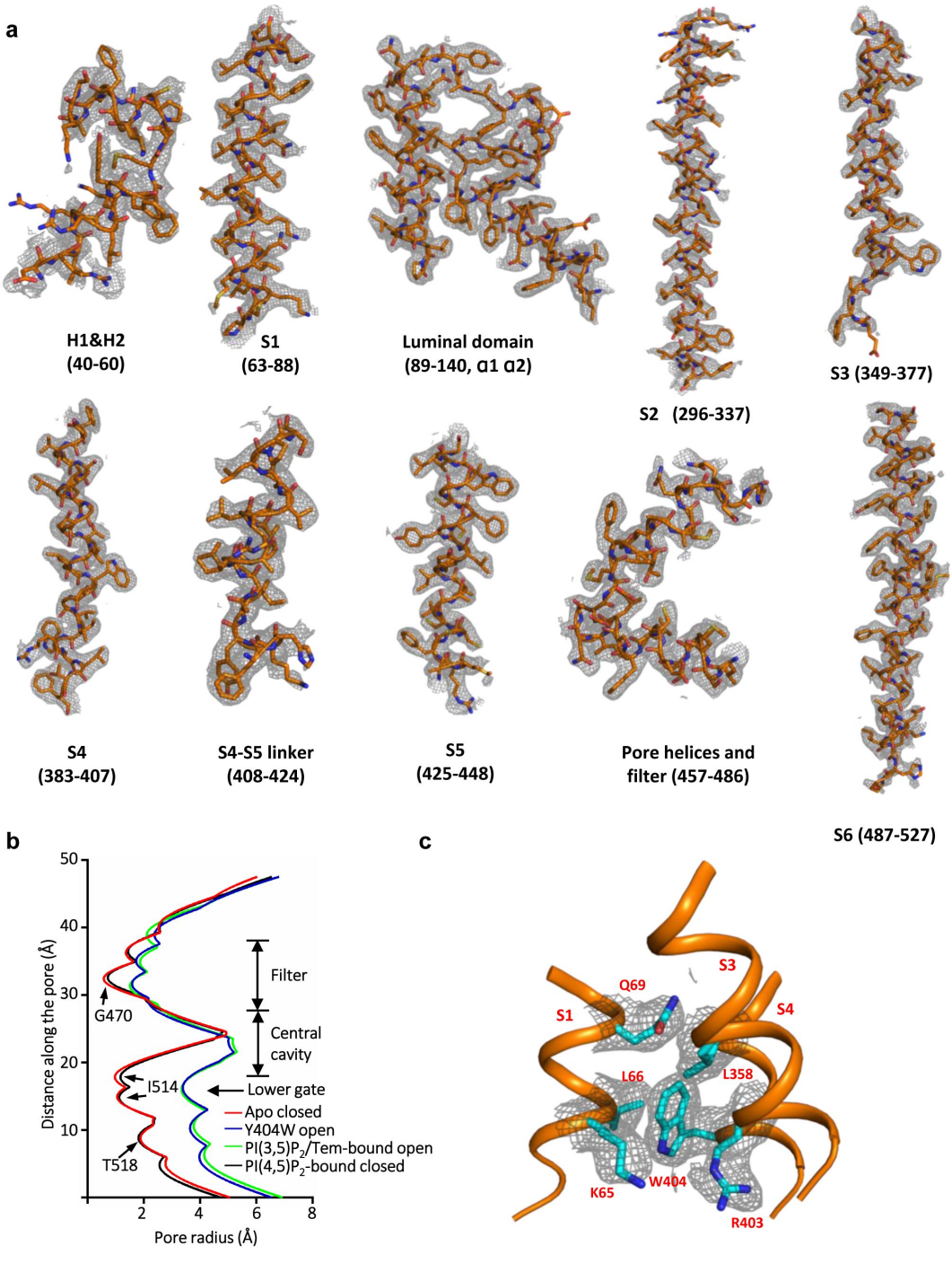

Figure supplement 3

Sample density maps of Y404W and pore radius:

(a) Sample density maps of the Y404W open TRPML1 structure contoured at 4 σ. (b) Pore radius along the central axis in the open and closed states. PDB codes for apo closed and PI(3,5)P_2/Tem-bound open are 7SQ8 and 7SQ9, respectively. (c) EM density map surrounding W404 region shown in grey mesh and contoured at 4σ, key W404-interacting residues are shown in cyan. The local resolution of this region is 3.2 Å.

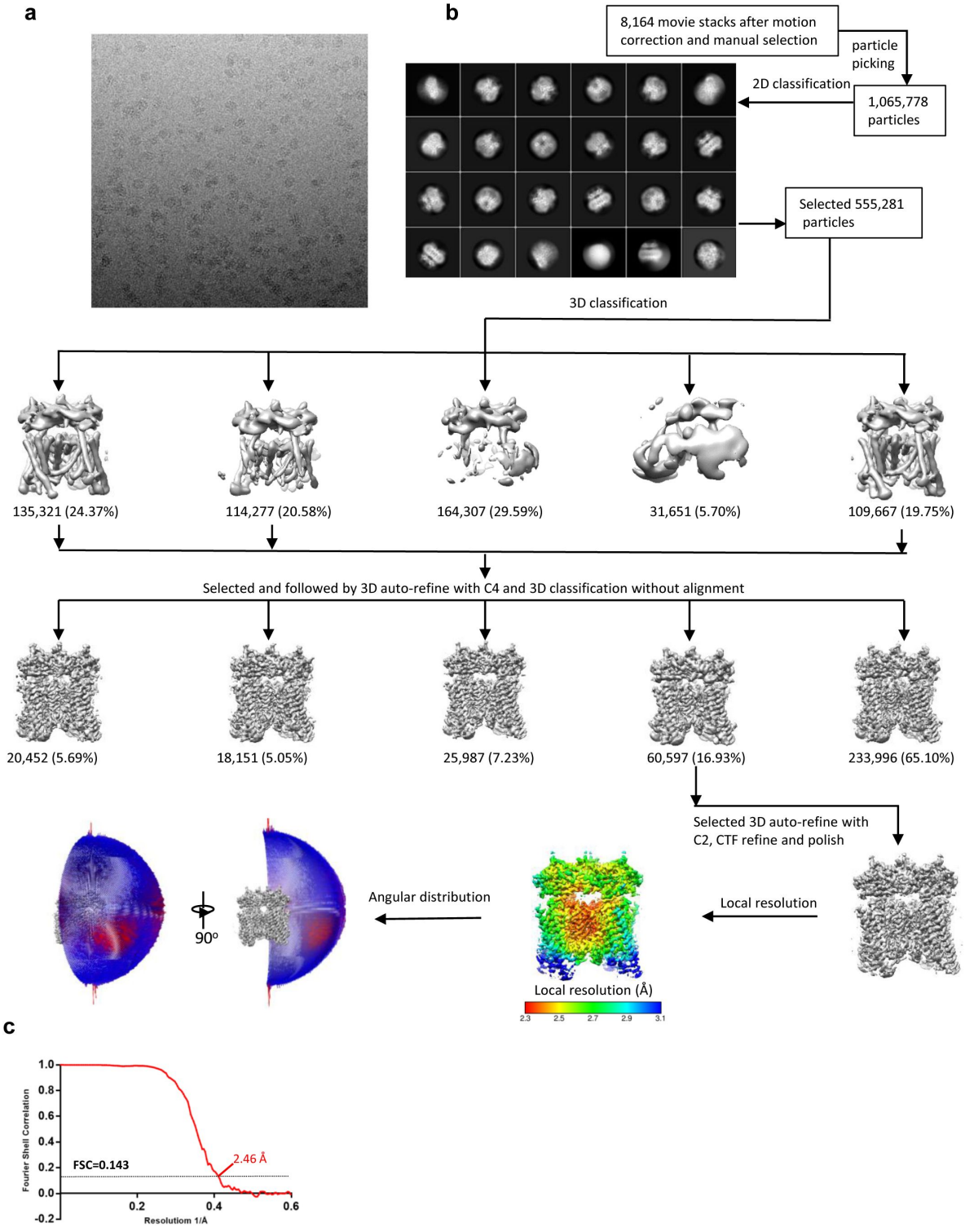

Figure supplement 4

Cryo-EM data processing scheme of the TRPML1 sample prepared in the presence of PI(4,5)P_2.

(a) Representative micrograph. (b) Flow chart of the cryo-EM data processing procedure and the Euler angle distribution of particles used in the final three-dimensional reconstruction. Selected 2D class averages are shown. The final structure represent an open state. (c) Fourier Shell Correlation curves showing the overall resolution at FSC=0.143.

Figure supplement 5

Sample density maps of the PI(4,5)P_2-bound closed TRPML1 structure contoured at 4 σ.

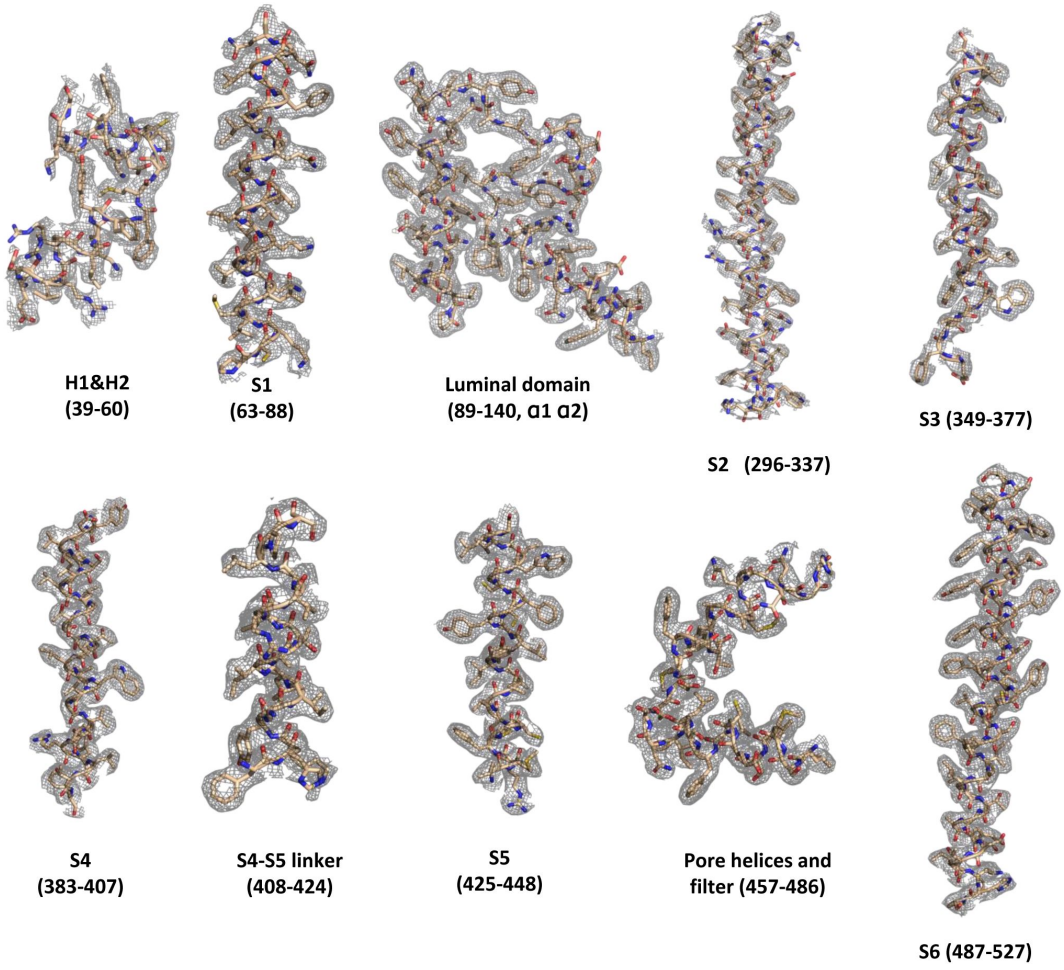

Figure supplement 6

Sphingomyelin (cyan) binding overlaps with that of agonist ML-SA1 (yellow), rapamycin analog Tem (magenta), or antagonist ML-SI3 (green).

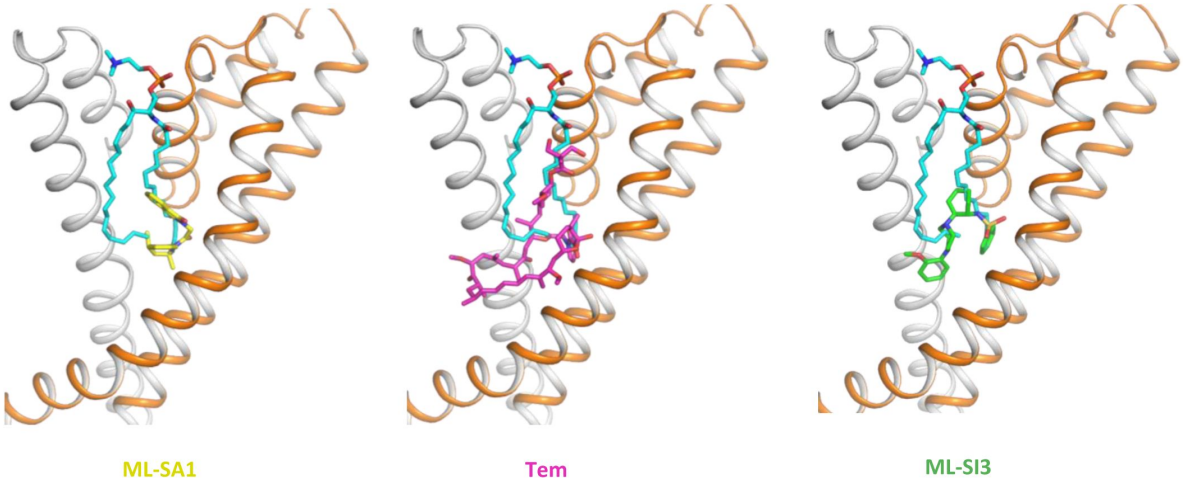

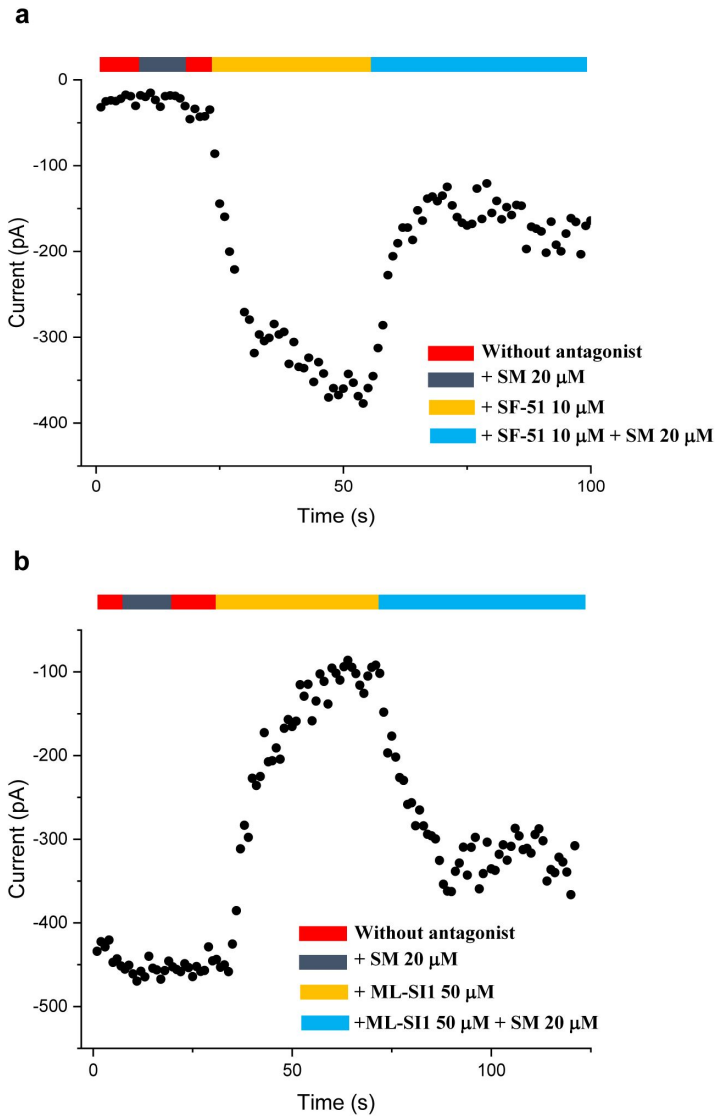

Figure supplement 7

Time course plots of sphingomyelin affected TRPML1 current amplitudes.

(a) Sphingomyelin inhibition effect on SF-51-activated wild-type TRPML1. (b) SM activation effect on ML-SI1-inhibited Y404W mutant. Currents shown in (a) and (b) were recorded at -140mV using patch clamp in whole-cell configuration with pH 4.6 in the bath solution as the adverse effect of SM on agonist or antagonist is subtle and is measurable only at low luminal pH.

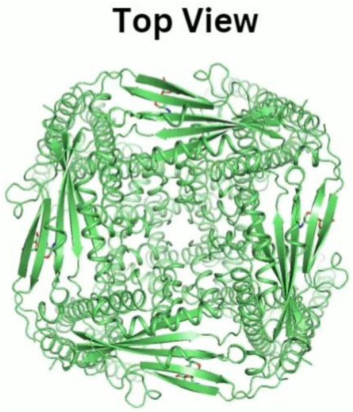

Movie supplement 1.

Conformational changes between open and closed TRPML1

References

Adams PD *et al.* (2010) **PHENIX: a comprehensive Python-based system for macromolecular structure solution** *Acta Crystallogr D Biol Crystallogr* **66**:213–221

Bargal R, Avidan N, Ben-Asher E, Olender Z, Zeigler M, Frumkin A, Raas-Rothschild A, Glusman G, Lancet D, Bach G (2000) **Identification of the gene causing mucolipidosis type IV** *Nat Genet* **26**:118–123

Bassi MT, Manzoni M, Monti E, Pizzo MT, Ballabio A, Borsani G (2000) **Cloning of the gene encoding a novel integral membrane protein, mucolipidin-and identification of the two major founder mutations causing mucolipidosis type IV** *Am J Hum Genet* **67**:1110–1120

Chen CC *et al.* (2014) **A small molecule restores function to TRPML1 mutant isoforms responsible for mucolipidosis type IV** *Nat Commun* **5**

Chen Q, She J, Zeng W, Guo J, Xu H, Bai X-c, Jiang Y (2017) **Structure of mammalian endolysosomal TRPML1 channel in nanodiscs** *Nature* **550**:415–418

Chen VB, Arendall WB, Headd JJ, Keedy DA, Immormino RM, Kapral GJ, Murray LW, Richardson JS, Richardson DC (2010) **MolProbity: all-atom structure validation for macromolecular crystallography** *Acta Crystallogr D Biol Crystallogr* **66**:12–21

Dong XP, Cheng X, Mills E, Delling M, Wang F, Kurz T, Xu H (2008) **The type IV mucolipidosis-associated protein TRPML1 is an endolysosomal iron release channel** *Nature* **455**:992–996

Dong XP *et al.* (2010) **PI(3,5)P(2) controls membrane trafficking by direct activation of mucolipin Ca(2+) release channels in the endolysosome** *Nat Commun* **1**

Dong XP, Wang X, Shen D, Chen S, Liu M, Wang Y, Mills E, Cheng X, Delling M, Xu H (2009) **Activating mutations of the TRPML1 channel revealed by proline-scanning mutagenesis** *J Biol Chem* **284**:32040–32052

Emsley P, Lohkamp B, Scott WG, Cowtan K (2010) **Features and development of Coot** *Acta Crystallogr D Biol Crystallogr* **66**:486–501

Fine M, Schmiege P, Li X (2018) **Structural basis for PtdInsP(2)-mediated human TRPML1 regulation** *Nat Commun* **9**

Gan N, Han Y, Zeng W, Wang Y, Xue J, Jiang Y (2022) **Structural mechanism of allosteric activation of TRPML1 by PI(3,5)P(2) and rapamycin** *Proc Natl Acad Sci U S A*

Gan N, Jiang Y (2022) **Structural biology of cation channels important for lysosomal calcium release** *Cell Calcium* **101**

Grimm C, Cuajungco MP, van Aken AF, Schnee M, Jörs S, Kros CJ, Ricci AJ, Heller S (2007) **A helix-breaking mutation in TRPML3 leads to constitutive activity underlying deafness in the varitint-waddler mouse** *Proc Natl Acad Sci U S A* **104**:19583–19588

Grimm C, Jörs S, Saldanha SA, Obukhov AG, Pan B, Oshima K, Cuajungco MP, Chase P, Hodder P, Heller S (2010) **Small molecule activators of TRPML3** *Chem Biol* **17**:135–148

Henderson R *et al.* (2012) **Outcome of the first electron microscopy validation task force meeting** *Structure* **20**:205–214

Kilpatrick BS, Yates E, Grimm C, Schapira AH, Patel S (2016) **Endo-lysosomal TRP mucolipin-1 channels trigger global ER Ca2+ release and Ca2+ influx** *J Cell Sci* **129**:3859–3867

Kim HJ, Li Q, Tjon-Kon-Sang S, So I, Kiselyov K, Muallem S (2007) **Gain-of-function mutation in TRPML3 causes the mouse Varitint-Waddler phenotype** *J Biol Chem* **282**:36138–36142

LaPlante JM, Falardeau J, Sun M, Kanazirska M, Brown EM, Slaugenhaupt SA, Vassilev PM (2002) **Identification and characterization of the single channel function of human mucolipin-1 implicated in mucolipidosis type IV, a disorder affecting the lysosomal pathway** *FEBS Lett* **532**:183–187

Morales-Perez CL, Noviello CM, Hibbs RE (2016) **Manipulation of Subunit Stoichiometry in Heteromeric Membrane Proteins** *Structure* **24**:797–805

Nagata K, Zheng L, Madathany T, Castiglioni AJ, Bartles JR, García-Añoveros J (2008) **The varitint-waddler (Va) deafness mutation in TRPML3 generates constitutive, inward rectifying currents and causes cell degeneration** *Proc Natl Acad Sci U S A* **105**:353–358

Nakane T *et al.* (2020) **Single-particle cryo-EM at atomic resolution** *Nature* **587**:152–156

Nilius B, Owsianik G, Voets T, Peters JA (2007) **Transient receptor potential cation channels in disease** *Physiol Rev* **87**:165–217

Pettersen EF, Goddard TD, Huang CC, Couch GS, Greenblatt DM, Meng EC, Ferrin TE (2004) **UCSF Chimera--a visualization system for exploratory research and analysis** *J Comput Chem* **25**:1605–1612

Prat Castro S, Kudrina V, Jaślan D, Böck J, Scotto Rosato A, Grimm C (2022) **Neurodegenerative Lysosomal Storage Disorders: TPC2 Comes to the Rescue!** *Cells* **11**

Samie M *et al.* (2013) **A TRP channel in the lysosome regulates large particle phagocytosis via focal exocytosis** *Dev Cell* **26**:511–524

Scheres SH (2012) **RELION: implementation of a Bayesian approach to cryo-EM structure determination** *J Struct Biol* **180**:519–530

Schmiege P, Fine M, Blobel G, Li X (2017) **Human TRPML1 channel structures in open and closed conformations** *Nature* **550**:366–370

Schmiege P, Fine M, Li X (2021) **Atomic insights into ML-SI3 mediated human TRPML1 inhibition** *Structure*

Schuchman EH (2010) **Acid sphingomyelinase, cell membranes and human disease: lessons from Niemann-Pick disease** *FEBS Lett* **584**:1895–1900

Scotto Rosato A *et al.* (2019) **TRPML1 links lysosomal calcium to autophagosome biogenesis through the activation of the CaMKKβ/VPS34 pathway** *Nature Communications* **10**

Shen D *et al.* (2012) **Lipid storage disorders block lysosomal trafficking by inhibiting a TRP channel and lysosomal calcium release** *Nat Commun* **3**

Slotte JP (2013) **Biological functions of sphingomyelins** *Prog Lipid Res* **52**:424–437

Smart OS, Neduvelil JG, Wang X, Wallace BA, Sansom MS (1996) **HOLE: a program for the analysis of the pore dimensions of ion channel structural models** *J Mol Graph* **14**:354–360

Sun M *et al.* (2000) **Mucolipidosis type IV is caused by mutations in a gene encoding a novel transient receptor potential channel** *Hum Mol Genet* **9**:2471–2478

Venkatachalam K, Wong CO, Zhu MX (2015) **The role of TRPMLs in endolysosomal trafficking and function** *Cell Calcium* **58**:48–56

Vergarajauregui S, Puertollano R (2006) **Two di-leucine motifs regulate trafficking of mucolipin-1 to lysosomes** *Traffic* **7**:337–353

Xu H, Delling M, Li L, Dong X, Clapham DE (2007) **Activating mutation in a mucolipin transient receptor potential channel leads to melanocyte loss in varitint-waddler mice** *Proc Natl Acad Sci U S A* **104**:18321–18326

Zhang K (2016) **Gctf: Real-time CTF determination and correction** *J Struct Biol* **193**:1–12

Zhang X *et al.* (2019) **Rapamycin directly activates lysosomal mucolipin TRP channels independent of mTOR** *PLoS Biol* **17**

Zhang X, Li X, Xu H (2012) **Phosphoinositide isoforms determine compartment-specific ion channel activity** *Proc Natl Acad Sci U S A* **109**:11384–11389

Zheng SQ, Palovcak E, Armache JP, Verba KA, Cheng Y, Agard DA (2017) **MotionCor2: anisotropic correction of beam-induced motion for improved cryo-electron microscopy** *Nat Methods* **14**:331–332

Zivanov J, Nakane T, Forsberg BO, Kimanius D, Hagen WJ, Lindahl E, Scheres SH (2018) **New tools for automated high-resolution cryo-EM structure determination in RELION-3** *Elife*

Editors

Reviewing Editor
László Csanády
Semmelweis University, Budapest, Hungary

Senior Editor
Kenton Swartz
National Institute of Neurological Disorders and Stroke, Bethesda, United States of America

Joint Public Review:

TRPML1 functions as a lysosomal ion channel whose variants are associated with lysosomal storage disorder mucolipidosis type IV. Understanding the structure and function of sites involved in the allosteric control TRPML1 may provide new molecular moieties to target with prototypic drugs.

Gan et al provide the first high resolution cryo-EM structure of a mutant (Y404W) TRPML1 channel in the open state without any activating ligands. This new structure demonstrates how a mutation at a site some distance away from the pore can influence channel gating. The authors provide compelling electrophysiology evidence which supports the proposed Y404W gain of function effect.

The authors propose an allosteric mechanism whereby the engineered W404 sidechain provides extra van der Waals contacts within a pocket surrounded by helices of the voltage sensor-like domain (VSLD) and causes S4 bending which in turn opens the pore through the S4-S5 linker. Conversely, the authors functionally demonstrate that an alanine mutation at this site causes a loss of function. Although the authors do not provide a structure of the Y404A mutant, they propose that the alanine substitution disrupts the sidechain packing and likely destabilizes the open conformation.

TRPML1 channels are regulated by PIP2 species in the cell. In the lysosomal membrane, PI(3,5)P2 activates the channel, whereas in the plasma membrane PI(4,5)P2 inhibits it. Towards understanding its lipid regulation, the authors solve a cryo-EM structure of TRPML1 bound to PI(4,5)P2 in the closed state and provide functional evidence that PI(4,5)P2 occupancy inhibits TRPML1 currents.

Within this same structure, the authors observe a density which may be attributed to sphingomyelin (or possibly phosphocholine). Using electrophysiology on WT and Y404W channels, the authors report an antagonist effect of sphingomyelin on TRPML1 currents.

Taken together, the study provides convincing evidence for a gating (opening/closing) mechanism of the TRPML1 pore which can be allosterically regulated by altered side-chain packing and by lipid interactions within the VSLD.

https://doi.org/10.7554/eLife.100987.2.sa1

Author response:

The following is the authors' response to the original reviews.

> ***Reviewer #1 (Public Review):***
>
> *In their manuscript, Gan and colleagues identified a functional critical residue, Tyr404, which when mutated to W or A results in GOF and LOF of TRPML1 activity, respectively. In addition, the authors provide a high-resolution structure of TRPML1 with PI(4,5)P2 inhibitor. This high-resolution structure also revealed a bound phospholipid likely sphingomyelin at the agonist/antagonist site, providing a plausible explanation for sphingomyelin inhibition of TRPML1.*
>
> *This is an interesting study, revealing valuable additional information on TRPML1 gating mechanisms including effects on endogenous phospholipids on channel activity. The provided data are convincing. Some major open questions remain. The work will be of interest to a wide audience including industry researchers occupied with TRPML1 exploration as a drug target.*

We appreciate reviewer #1's positive comments and the specific points raised by this reviewer are addressed in our response to Recommendations For The Authors

> ***Reviewer #2 (Public Review):***
>
> *The transient receptor potential mucolipin 1 (TRPML1) functions as a lysosomal organelle ion channel whose variants are associated with lysosomal storage disorder mucolipidosis type IV. Understanding sites that allosterically control the TRPML1 channel function may provide new molecular moieties to target with prototypic drugs.*
>
> *Gan et al provide the first high-resolution cryo-EM structures of the TRPML1 channel (Y404W) in the open state without any activating ligands. This new structure demonstrates how a mutation at a site some distance away from the pore can influence the channel's conducting state. However, the authors do not provide a structural analysis of the Y404W pore which would validate their open-state claims. Nonetheless, Gan et al provide compelling electrophysiology evidence which supports the proposed Y404W gain of function effect. The authors propose an allosteric mechanism with the following molecular details- the Y404 to W sidechain substitution provides extra van der Waals contacts within the pocket surrounded by helices of the VSD-like domain and causes S4 bending which in turn opens to the pore through the S4-S5 linker. Conversely, the author functionally demonstrates that an alanine mutation at this site causes a loss of function. Although the authors do not provide a structure of the Y404A mutation, they propose that the alanine substitution disrupts the sidechain packing and likely destabilizes the open conformation. TRPM1 channels are regulated by PIP2 species, which is related to their cell function. In the membrane of lysosomes, PI(3,5)P2 activates the channel, whereas PI(4,5)P2 found in the plasma membrane has inhibitory effects. To understand its lipid regulation, the authors solved a cryo-EM structure of TRPM1 bound to PI(4,5)P2 in its presumed closed state. Again, while the provided functional evidence suggests that PI(4,5)P2 occupancy inhibits TRPML1 current, the authors do not provide analysis of the pore which would support their closed state assertion. Within this same structure, the authors observe a density that may be attributed to sphingomyelin (or possibly phosphocholine). Using electrophysiology of WT and the Y404W channels, the authors report sphingomyelins antagonist effect on TRPML1 currents under low luminal (external) pH. Taken together, the results described in Gan et al provide compelling evidence for a gating (open, closed) mechanism of the TRPML1 pore which can be allosterically regulated by altered packing and lipid interactions within the VSDL.*

We appreciate reviewer #2's positive comments and constructive suggestions. We functionally demonstrated that the Y404A mutant is more stable in the closed state. We did not pursue the structure of this mutant as we expect its structure will be the same as the apo closed TRPML1. To verify the open conformation of the Y404W mutant and the closed conformation of PI(4,5)P2 –bound TRPML1, we analyzed the pore radii of our structures in the revision as suggested by the reviewer and compared them with open and closed pores from previously determined TRPML1. Some specific points raised by this reviewer are addressed in our response to Recommendations For The Authors

> ***Reviewer #1 (Recommendations For The Authors):***
>
> *(1) Mutations in TRPML1 cause Mucolipidosis type IV. One patient mutation reported earlier (Chen et al., 2014 https://pubmed.ncbi.nlm.nih.gov/25119295/) to be a LOF mutation is R403C. This mutation resides just next to the here-identified Y404 position which can be converted in either LOF or GOF. Another patient mutation, F408del (also reported previously: (Chen et al., 2014 https://pubmed.ncbi.nlm.nih.gov/25119295/)) results in a mild activity reduction, in particular of the PI(3,5)P2 effect. Can the authors please discuss their findings in the context of the reported literature on these patient mutations and provide explanations as to why this part of the TRPML1 protein seemingly is such a hotspot for mutations affecting channel activity and how they explain this*

> *based on their structural evidence? What characteristics would be required for a small molecule agonist of TRPML1 in order to elicit larger activation in these patient LOF mutations if possible?*

We thank the reviewer for highlighting these mutations identified in human patients. R403 appears to play two key roles. Firstly, its side chain participates in stabilizing Y404 in the open state. Secondly, as demonstrated in our previous study on TRPML1 (PMID: 35131932), the R403 side chain points towards the PI(3,5)P2 binding pocket, where it forms a critical salt bridge with the C3 phosphate group in the open state. Therefore, R403C mutation likely abolishes PI(3,5)P2 activation and also destabilizes the open state, resulting in the loss of function of the channel. We have expanded our discussion on this mutation in the revision. F408 is positioned at the junction between S4 and the S4-S5 linker. Its deletion mutation could change the stability or the folding of the protein. It is difficult to speculate the exact cause of the F408Δ LOF based on the TRPML1 structure. We don't feel the effect of this mutation is relevant to the findings of this study.

> *(2) The authors used ML-SA1 only as a basis for their claims. Could they possibly provide some key data also on alternative small molecule agonists such as SF-51 and/or MK6-83?*

We thank the reviewer for this suggestion. The TRPML1 agonists such as ML-SA1 (derived from SF-51) and MK6-83 have been well characterized in previous studies. In our study of sphingomyelin effect on TRPML1 activity, we used SF-51 to activate the channel (Figure 4b). The goal of our study is to demonstrate that agonist and antagonist can still allosterically regulate the LOF Y404A and GOF Y404W mutant channels, respectively, and their competition with sphingomyelin. We chose ML-SA1 in our experiment simply because it has been a commonly used TRPML1 agonist and its binding has been structurally defined, allowing us to compare various TRPML1 structures with different ligands. We don't feel the use of other agonists would add extra information to our findings.

> *(3) Sphingomyelin effects on TRPML1 have been confirmed by other groups as well (see e.g. Prat Castro et al., 2022 https://pubmed.ncbi.nlm.nih.gov/36139381/ Fig.3. Interestingly TPC2 seems unaffected by sphingomyelin albeit it is also activated by PI(3,5)P2. Can the authors provide possibly some modeling and/or cryoEM data on TPC2 with sphingomyelin to potentially explain why TPC2 is seemingly unaffected by sphingomyelin?*

We appreciate the reviewer for providing additional evidence of sphingomyelin's effects on TRPML1 and have included the reference in revision. The binding site and activation mechanism of PI(3,5)P2 are different between TPC2 and TRPML1. It is beyond the scope of this study and also too speculative to model sphingomyelin binding (if any) in TPC2 to explain its lack of effect on TPC2 activity.

> ***Reviewer #2 (Recommendations For The Authors):***
>
> *The findings from Gan et al provide structural insights into the allosteric regulation of TRPML1 channel gating. The authors have provided compelling and hard-won cryo-EM structural evidence of the channel regulation by PI4,5P2 and at sites that pack the gating pore of the VSDL (S4). However, as noted in the public review, the analysis of the cryo-EM structures that would support claims of open and closed channel states is woefully lacking. Additional information related to the functional results is required to evaluate the activation and inhibition kinetic effect of lipids and pharmacological agents used to support their allosteric mechanism of TRPML1 gating.*
>
> *Major concerns:*

> *(a) At the very least, the pore domains of the new channels (PDB 9CBZ and 9CC2) should be analyzed using the HOLE (or other) programs to estimate the distances along the ion-conducting pathway - are the structures wide enough to support the passage of hydrated or partially hydrated cations? Additional figure panels should provide this comparative analysis.*

We thank the reviewer for this valuable suggestion. We have added a figure (Figure Supplement 3b) of pore domain radius analysis using the HOLE program in the revision and have also included the radius comparison with previous determined open and closed TRPML1 structures.

> *(b) At the very least, all current traces (Figures 1C, 1D, 1E, 4B, 4C) should be accompanied by time course plots of current amplitudes. It is impossible to evaluate the authors' claims of lipid and drug effects on TRPML1 channels without this information.*

The corresponding time course plots of current amplitudes have now been included in the revision as Figure Supplement 1 and 7.

> *(c) Regarding the gain of function Y404W mutation structure, the authors' allosteric mechanistic hypothesis centers on side chain packing details within the VSD-like domain S4 (which in turn opens the pore through the S4-S5 linker). However, the local resolution within the structures at this site is not described. To assess the veracity of these claims, at the very least, authors should provide electron density maps of this region, either in Figure 2 or in Figure Supplement 4.*

We have included the electron density map and local resolution information surrounding the W404 residue from the Y404W GOF mutant structure in the revision as Figure Supplement 3c.

> *Minor concerns:*
>
> *(d) Additional evidence related to the identity of the pore domain-associated lipid density (PC or sphingomyelin), and its channel regulation would improve the manuscript. The authors examine sphingomyelin, but what is the functional impact of PC on TRPML1 currents? While this is suggested, it is at the authors' discretion whether or not to carry out this analysis.*

We thank the reviewer for raising this question. Adding extra PC has no effect on TRPML1 activity. This is expected since PC is the major lipid component of the membrane.

> *(e) The manuscript is well written. However, a few errors were noted while reviewing this draft.*
>
> *i. Line 138, (Figure F&G).*
>
> *ii. Line 66, "signaling transduction".*

These errors have now been corrected.

https://doi.org/10.7554/eLife.100987.2.sa0